Liquid Crystals
Publication details, including instructions for authors and subscription information:
http://www.informaworld.com/smpp/title~content=t713926090

Side group functionalized liquid crystalline polymers and blends VIII. Nematic and SmA_{re} phase formation in hydrogen-bonded blends of smectic side group LC polymers and a low molar mass dopant

E. B. Barmatov; A. P. Filippov; V. P. Shibaev

Online publication date: 06 August 2010

To cite this Article Barmatov, E. B. , Filippov, A. P. and Shibaev, V. P.(2001) 'Side group functionalized liquid crystalline polymers and blends VIII. Nematic and SmA_{re} phase formation in hydrogen-bonded blends of smectic side group LC polymers and a low molar mass dopant', Liquid Crystals, 28: 4, 511 — 523
To link to this Article: DOI: 10.1080/02678290010022551
URL: http://dx.doi.org/10.1080/02678290010022551

LIQUID CRYSTALS, 2001, VOL. 28, NO. 4, 511–523

Side group functionalized liquid crystalline polymers and blends VIII. Nematic and SmA_{re} phase formation in hydrogen-bonded blends of smectic side group LC polymers and a low molar mass dopant

E. B. BARMATOV*, A. P. FILIPPOV†, V. P. SHIBAEV

Chemistry Department, Moscow State University, 119899 Moscow, Russia
†Institute of Macromolecular Compounds, Russian Academy of Sciences, Bolshoi pr. 31, 199004 St.-Petersburg, Russia

(*Received 29 June 2000; in final form 11 October 2000; accepted 28 October 2000*)

Hydrogen-bonded blends based on smectic side group functionalized LC copolymers containing 4-alkyloxybenzoic acid fragments (proton donor) and a non-mesogenic low molecular mass dopant 4-cyanophenyl pyridine-4-carboxylateor 4-methoxyphenyl-d_4 pyridine-4-carboxylate (proton acceptor) were obtained. The blends containing 10–35 mol % of low molecular weight dopant form nematic (I–N–SmA) or re-entrant SmA phases (I–SmA–N–SmA_{re}). The temperature dependence of the order parameter S, the birefringence Δn, and the splay K_1 and bend K_3 elastic constants of the nematic phase were studied by ^{2}H NMR spectroscopy and the Fréedericksz method of threshold transitions in a magnetic field. A mechanism for the destruction of the SmA phase and the formation of the nematic phase in the hydrogen-bonded blends is suggested.

1. Introduction

In the last decade of our century in the liquid crystal field, great interest has arisen in the effect of hydrogen bonds and donor–acceptor and Coulomb interactions on the phase behaviour and properties of low molecular mass [1–5] and polymeric [5–7] LCs.

In our publications [8–11] we have developed an approach to the synthesis of new functionalized LC polymers based on the combination of monomer units of different nature and polarity in the same macromolecule. Functionalized LC polymers contain two types of side groups: mesogenic groups responsible for liquid crystalline phase formation, and functional groups of the acrylic or maleic types or derivatives of *n*-alkyloxybenzoic acids capable of hydrogen bonding. The scheme of such a functionalized macromolecule containing LC as functional copolymer fragments is shown below:

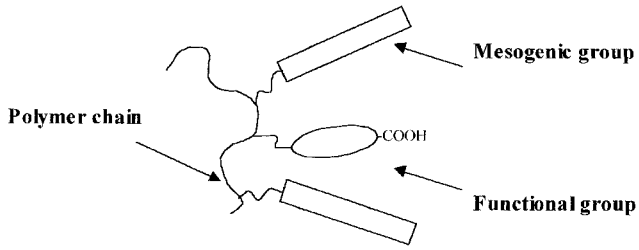

*Author for correspondence;
e-mail: barmatov@libro.genebee.msu.su

Functionalized LC polymers are suitable matrices for the controlled modification of polymer properties by their combination with low molar mass dopants containing chiral [9] or photochromic [5] groups.

The present paper deals with the hydrogen-bonded blends of functionalized LC polymers and low molar mass pyridine-containing **PyCN** and **PyOCH$_3$** dopants. Smectic copolymers **P3**, **P6**, and **P9** with acid group concentrations of 31–40 mol % were chosen as the functionalized LC matrices.

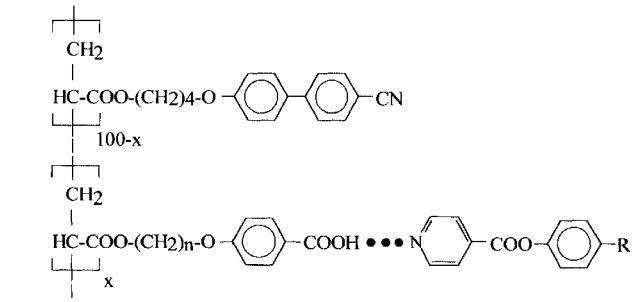

Functionalized LC copolymers **P3**, **P6** and **P9**:

$n = 3$; $x = 31$ mol % (**P3**)
$n = 6$; $x = 40$ mol % (**P6**)
$n = 9$; $x = 39$ mol % (**P9**)

Dopant Py***R*** (10–35 mol %):

R = CN (**PyCN**)
R = OCH_3 (**PyOCH3**)

Liquid Crystals ISSN 0267-8292 print/ISSN 1366-5855 online © 2001 Taylor & Francis Ltd
http://www.tandf.co.uk/journals
DOI: 10.1080/02678290010022551

The emphasis of this paper is on the following points:

(i) The preparation of new hydrogen-bonded blends of functionalized LC polymers **P3–P9** with low molar mass dopants **Py*R*** and the study of their structure and phase behaviour.
(ii) The study of the hydrogen bond formation in the blends.
(iii) The study of the orientational behaviour of the LC blends in a magnetic field and the determination of values of the order parameter S, birefringence Δn, and splay K_1 and bend K_3 elastic constants. It should be pointed out that we have used deuteriated dopant **PyOCH$_3$** that makes it possible to use NMR measurements to obtain information on the behaviour of the 'labelled' dopant and calculate the order parameter.

2. Experimental

The following monomers 4-(4′-cyanobiphenyl-4-yloxy)-butyl acrylate (**CB**), 4-(3-acryloyloxypropyl-1-oxy)benzoic acid (**A3**), 4-(6-acryloyloxyhexyl-1-oxy)benzoic acid (**A6**), and 4-(9-acryloyloxynonyl-1-oxy)benzoic acid (**A9**) were synthesized according to previously described procedures [9].

CB (Cr 93 I): ^{1}H NMR ($CDCl_3$): δ 7.97 (d, 2H, Ph, $J = 8.85$ Hz); 7.67 (d, 2H, Ph, $J = 8.55$ Hz); 7.62 (d, 2H, Ph, $J = 8.51$ Hz); 7.51 (d, 2H, Ph, $J = 8.81$ Hz); 6.35 (dd, 1H, C$\underline{H}_2$=CH−, $J = 1.65$, 17.65 Hz); 6.12 (dd, 1H, CH_2 = C$\underline{H}$−, $J = 10.3$, 17.31 Hz); 5.81 (dd, 1H, C$\underline{H}_2$=CH−, $J = 1.65$, 10.3 Hz); 4.21 (t, 2H, O−C$\underline{H}_2$); 4.02 (t, 2H, −C$\underline{H}_2$−O); 1.89 (4H, −C$\underline{H}_2$−C$\underline{H}_2$−).

A3 (Cr 109 I (N 103 I)): ^{1}H NMR ($CDCl_3$): δ 7.95 (d, 2H, Ph, $J = 8.82$ Hz); 6.93 (d, 2H, Ph, $J = 8.82$ Hz); 6.35 (dd, 1H, C$\underline{H}_2$=CH−, $J = 1.65$, 17.65 Hz); 6.12 (dd, 1H, CH_2 = C$\underline{H}$−, $J = 10.3$, 17.31 Hz); 5.81 (dd, 1H, C$\underline{H}_2$ = CH−, $J = 1.65$, 10.3 Hz); 4.3 (t, 2H, O−C$\underline{H}_2$−); 4.12 (t, 2H, −C$\underline{H}_2$−O); 2.13 (2H, −C$\underline{H}_2$−).

A6 (Cr 85 SmA 96 N 103 I): ^{1}H NMR ($CDCl_3$): δ 7.95 (d, 2H, Ph, $J = 8.82$ Hz); 6.93 (d, 2H, Ph, $J = 8.82$ Hz); 6.35 (dd, 1H, C$\underline{H}_2$=CH−, $J = 1.65$, 17.65 Hz); 6.12 (dd, 1H, CH_2=C$\underline{H}$−, $J = 10.3$, 17.31 Hz); 5.81 (dd, 1H, C$\underline{H}_2$=CH−, $J = 1.65$, 10.3 Hz); 4.3 (t, 2H, O−C$\underline{H}_2$−); 4.12 (t, 2H, −C$\underline{H}_2$−O); 1.3–1.9 (8H, −C$\underline{H}_2$−).

A9 (Cr SmA 97 N 105 I): ^{1}H NMR ($CDCl_3$): δ 7.95 (d, 2H, Ph, $J = 8.82$ Hz); 6.93 (d, 2H, Ph, $J = 8.82$ Hz); 6.35 (dd, 1H, C$\underline{H}_2$=CH−, $J = 1.65$, 17.65 Hz); 6.12 (dd, 1H, CH_2=C$\underline{H}$−, $J = 10.3$, 17.31 Hz); 5.81 (dd, 1H, C$\underline{H}_2$=CH−, $J = 1.65$, 10.3 Hz); 4.31 (t, 2H, O−C$\underline{H}_2$−); 4.12 (t, 2H, −C$\underline{H}_2$−O); 1.2–1.9 (14H, −C$\underline{H}_2$−).

Copolymers **P3**, **P6**, and **P9** were obtained by free radical copolymerization of monomers **CB** and **A3** (**A6**, **A9**) in absolute THF; AIBN was used as initiating agent. The as-synthesized copolymers were purified by repeated precipitation from THF solutions by hexane. The compositions of the copolymers (see the table) were determined by ^{1}H NMR spectroscopy, comparing the integral intensity of the aromatic protons of the mesogenic group **CB** and the oxybenzoic ring of **A3**, **A6** and **A9**.

The relative molecular masses of the polymers were determined by gel permeation chromatography (GPC) using a GPC-2 Waters instrument equipped with an LC-100 column oven and a Data Modul-370 data station (see the table). Measurements were made with a UV detector, THF as solvent (1 ml min^{-1}, 25°C), a set of PL columns of 100, 500 and 1000 Å, and a calibration plot constructed with (poly)styrene standards (M_w = 1000–430 500).

The dopants 4-cyanophenyl pyridine-4-carboxylate (**PyCN**, m.p. 114–115°C) and 4-methoxyphenyl-d_4 pyridine-4-carboxylate (**PyOCH$_3$**, m.p. 89–90°C) were prepared by ordinary synthetic procedures. According to ^{1}H NMR spectroscopy, the degree of deuteriation was 95.0 ± 0.4% for **PyOCH$_3$**. The blends of the copolymers with **PyCN** or **PyOCH$_3$** were prepared by dissolution of the components with various compositions in THF and drying down in vacuum.

Phase transitions in the synthesized copolymers and blends were studied by differential scanning calorimetry (DSC) at a scanning rate of 10°C min^{-1} from −10 to 150°C under nitrogen. The DSC cell was calibrated with indium. Polarizing optical microscopy (POM) was performed using a Mettler FP90 thermal analyser and a Zeiss polarizing microscope. X-ray diffraction (XRD) analysis was carried out using a URS-55 instrument (Ni-filtered CuK_α radiation). The IR spectra were recorded

Table. Molecular mass characteristics, composition and phase behaviour of the functionalized LC copolymers **P3**, **P6** and **P9**.

Sample	Portions of functional monomer units **A3**, **A6** and **A9** in the LC copolymer/mol %	M_w	M_w/M_n	Phase behaviour/°C
P3	31	5300	1.8	Glass 49 SmA 125–140 I
P6	40	4800	1.8	Glass 30 SmA 105–115 I
P9	39	6200	1.7	Glass 38 SmA 110–120 I

using an FTIR spectrometer (Biorad FTS 6000) with a hot stage. ^{2}H NMR spectroscopy measurements were performed in a field of 11.7 T at a frequency of 76.75 MHz (Bruker MSL 500 spectrometer). Single pulse excitation without proton decoupling was used.

The orientational elastic deformations and birefringence Δn of nematic blends were investigated by the Fréedericksz method of threshold transitions in a magnetic field [12–14]. The LC blends were placed between the spherical and planar optical surfaces. The quartz glasses and lenses used had their surfaces treated with concentrated sulphuric acid followed by washing with distilled water. This treatment enabled us to obtain homeotropic textures for the copolymers in which the nematic director is normal to the support surface. To prepare planar textures (with the director aligned parallel to the support surface), we used the usual procedure of rubbing the quartz glass and lens surfaces with a cloth. The sample was observed by POM in a parallel light beam normal to the deforming field. Photographs of the deformation patterns were taken.

On exposure to the magnetic field applied normal to the director, orientational elastic deformations appear in the nematic. They are of a threshold character and give a minimum critical magnetic field $\mathbf{H}_c$ at which deformation is possible for a nematic layer with a thickness z_c. According to the Fréedericksz law, the product $z_c\mathbf{H}_c$ determines the ratio of the elastic constant to the specific diamagnetic anisotropy $K_i/\Delta\chi$ [12]:

$$z_c\mathbf{H}_c = \pi(K_i/\Delta\chi)^{1/2} \quad (1)$$

where $i = 1$ for the deformation of planar layers and $i = 3$ for the deformation of homeotropic layers.

For an undeformed planar nematic layer, concentric interference rings (lines of equal thickness) are observed. For these rings, the optical phase difference is proportional to the wavelength λ of the incident light, which makes it possible to determine easily the birefringence of the nematic layer:

$$\Delta n = m\lambda/z \quad (2)$$

where m is the order of the dark interference ring corresponding to a layer thickness z. The precision of Δn determination is approximately 3% and that of the splay K_1 and bend K_3 elastic constants is 5–10%.

3. Results and discussion

3.1. *Induction of the nematic phase in the hydrogen-bonded blends*

Figure 1 (*a–d*) shows phase diagrams of blends of copolymers **P3**, **P6**, and **P9** with dopants **PyCN** and **$PyOCH_3$**. It can be seen that the incorporation of the low molar mass dopants into the smectic matrices leads to a change in their phase behaviour, in particular decreasing the clearing temperatures. Starting with a dopant concentration of ~10–15 mol %, the nematic phase is induced in all blends. Moreover, for the **P3-$PyOCH_3$** (*a*) and **P3-PyCN** (*b*) blends, the nematic phase is formed after the smectic phase with decreasing temperature. The following phase sequence is observed†: I–SmA–N–SmA_{re}.

The nematic phase in the **P3-$PyOCH_3$** blend is formed in the composition range 15–22 mol % of **$PyOCH_3$** dopant. Further increase in the percentage of **$PyOCH_3$** molecules causes degeneration of the induced nematic phase, and only the SmA phase is retained for the blends. In this case, over a relatively wide range of **$PyOCH_3$** dopant concentrations, the temperature range of the nematic phase 'pressed' between two SmA phases is virtually independent of blend composition. A somewhat different situation is observed for the **P3-PyCN** blend. With increasing dopant content (10–25 mol %), a tendency to stabilization of the temperatures of the N↔SmA_{re} transition is observed; the biphasic region I + SmA becomes wider, and the range of the nematic phase becomes narrower. Further increase (more than 25 mol %) in **PyCN** concentration is limited by the content of acid groups in the polymer **P3** (31 mol % of **A3** groups). Therefore, we were unable to study the evolution of phase behaviour of the blends at higher dopant contents.

The phase states of the LC copolymers and blends were investigated by POM, DSC, and XRD. The thermotropic behaviour of the copolymers **P3**, **P6** and **P9** and their blends was studied by DSC. Figure 2 shows the thermograms for copolymer **P3** and blends **P3-$PyOCH_3$** and **P3-PyCN** in the second scan regime. One broad endothermic peak with enthalpy, $\Delta H = 0.8$–$1.9\ J\ g^{-1}$ was detected. To characterize the broad endothermic peak, the optical polarization textures of the copolymers and blends were examined. The nematic phase forms a characteristic marble texture, figure 3 (*c*, *d*); the smectic phase forms bâtonnets or fan-shaped textures, figure 3 (*a*, *b*, *h*). The X-ray pattern of the magnetically

† In describing phase behaviour in **P3-PyR** blends, the authors encountered a dilemma. From the formal viewpoint, the designation of re-entrant smectic A phase (SmA_{re}) is introduced. On the other hand, the phase sequence may be written in another way: I–SmA–N_{re}–SmA_{re}. In this case the unusual character of the nematic phase is emphasized: this phase appears at a lower temperature than the phase with one-dimensional translational order (SmA). Being guided by this criterion, we called the nematic phase for the **P3-PyCN** blends in our first preliminary publication [11] as re-entrant. It should be noted that a similar phase sequence for side group LC polymers was recently detected [15]. At the same time the phase sequences most generally found for LC polymers are I–N–SmA–N_{re} [16] or I–N–SmA–N_{re}–SmX, where SmX is SmC [17] or SmF [18].

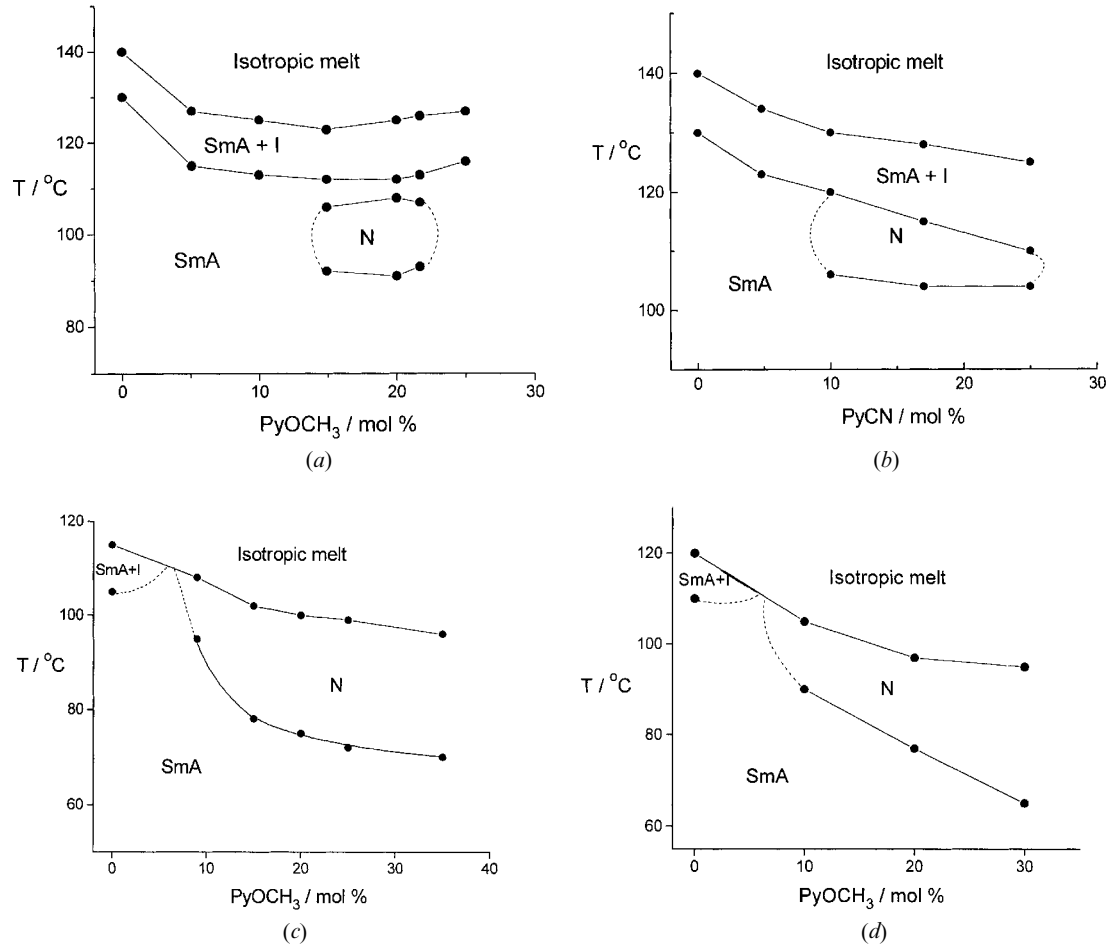

Figure 1. Phase diagrams for the blends **P3-PyOCH$_3$** (*a*), **P3-PyCN** (*b*), **P6-PyOCH$_3$** (*c*), and **P9-PyOCH$_3$** (*d*). Phase diagrams were constructed on the basis of polarizing optical microscopy.

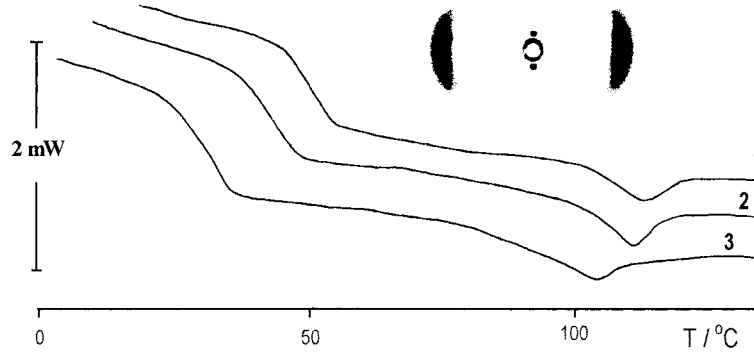

Figure 2. DSC curves for polymer **P3** (1), and blends **P3-PyCN-17** (2) and **P3-PyOCH$_3$-20** (3); the X-ray pattern is for the magnetically oriented blend **P3-PyCN-17** at room temperature.

oriented smectic phase shows small and wide angle reflections split in mutually perpendicular directions, which indicates the formation of the SmA phase at room temperature (figure 2).

It should be pointed out that in all blends macroscopic phase separation is absent. Prolonged annealing of the blends in the mesophase and in the isotropic melt does not lead to changes in the transition temperatures and phase states. The formation of blends of the LC polymers **P3**, **P6** and **P9** with the **Py*R*** dopants leads to the appearance of nematic and smectic phases. However, the **PyCN** and **PyOCH$_3$** dopants in the pure state are crystalline compounds with high melting enthalpies, $\Delta H = 46$ J g^{-1} (for **PyOCH$_3$**). The melting peaks of the

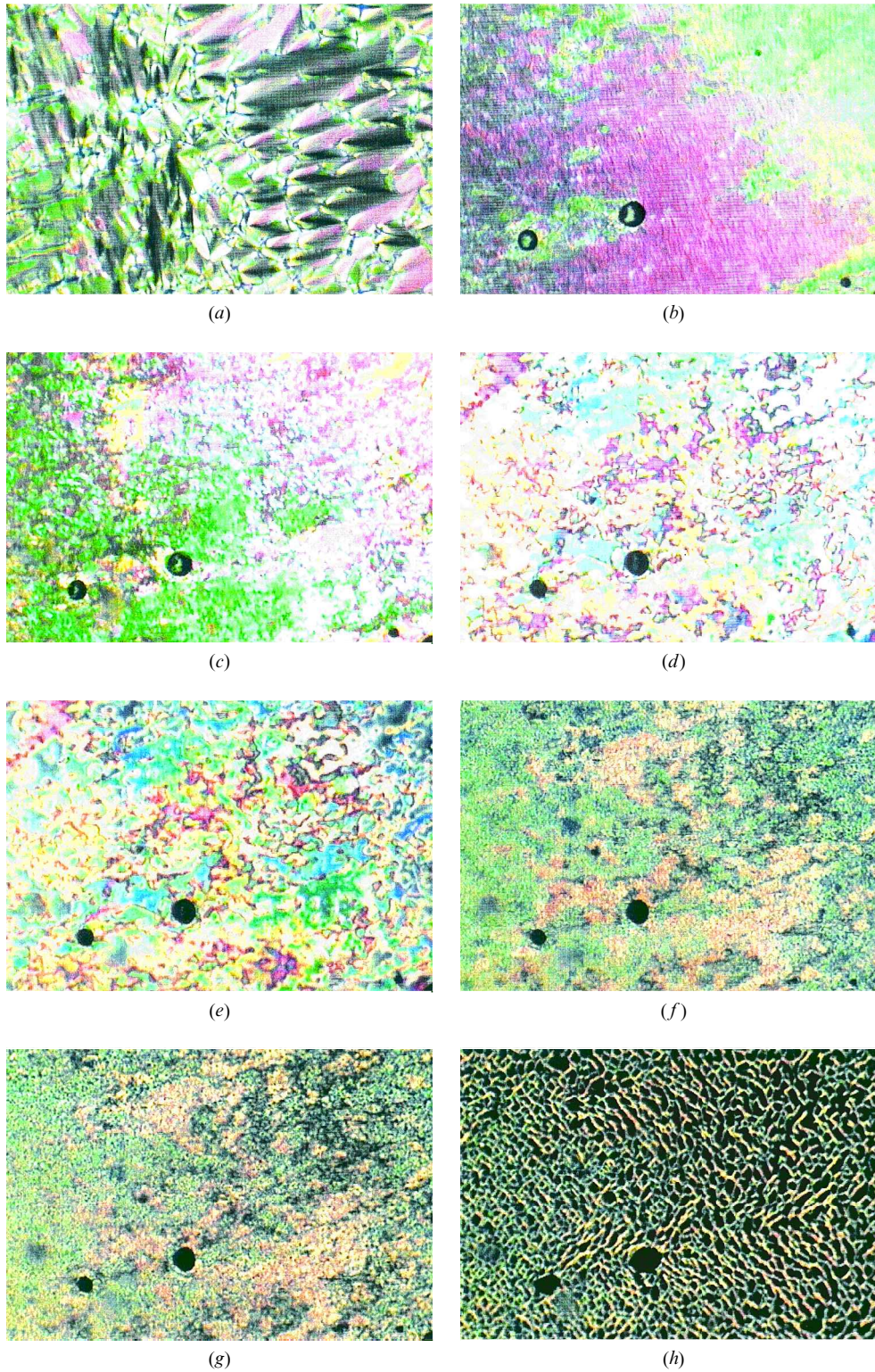

(*a*) (*b*) (*c*) (*d*) (*e*) (*f*) (*g*) (*h*)

Figure 3. Optical polarizing photomicrographs of the LC functionalized copolymer **P3** (*a*) and the blend **P3-PyOCH$_3$-20** (*b–h*) at different temperatures (°C): 30 (*a*), 70 (*b*), 85 (*c*), 100 (*d*), 106 (*e*), 108 (*f*), 110 (*g*) and 115 (*h*).

dopants are completely absent from the DSC curves of the blends and there are no characteristic crystalline peaks on their X-ray patterns. This indicates that dopant molecules are incorporated into the LC polymer matrix with the formation of a 'new' compound stabilized by intermolecular hydrogen bonds, figure 4 (*b*).

A detailed analysis of the character of hydrogen bonds in the macromolecules of the initial compounds and the blends was made on the basis of FTIR spectroscopy. Figure 5 shows the IR spectra of the functionalized LC copolymer **P3**, the dopant **PyOCH$_3$**, and the blend **P3-PyOCH$_3$**. It can be clearly seen that the range 1650–1800 cm^{-1} contains several overlapping bands assigned to stretching mode [$\nu_{C=O}$] of the carboxyl groups. We assign the band at 1682 cm^{-1} to COOH groups bound by hydrogen bonds, according to [19]. The ester group vibrations unfortunately overlap the band of the free carboxyl group. Hence, in further analysis of hydrogen bonding in the blends, the vibrational intensity of the bound carboxyl group $I[\nu_{C=O}]$ will be used. For samples of the LC copolymer and of the blend, the [$\nu_{C=O}$] band is shifted with temperature increasing (from 1682 to 1691 cm^{-1}). This relationship, as well as decreasing intensity of the [$\nu_{C=O}$] vibration (figure 6), shows that hydrogen bonds break with increasing temperature.

The maximum change in the [$\nu_{C=O}$] intensity takes place in the range of the SmA–I or N–SmA–I phase transitions. For the functionalized LC copolymer **P3**, a jump in the ratio $I[\nu_{C=O}]/I[\nu_{CN}]$ is observed during the melting of the SmA phase; this transition takes place over a broad temperature range (up to 25°C). For the **P3-PyOCH$_3$** blend the loss in intensity of the bound carboxyl group coincides with the limits of the nematic phase. The formation of the hydrogen bonds between **P3** and **PyOCH$_3$** is indicated by an increasing intensity of [$\nu_{C=O}$] bands (1682 cm^{-1}) as compared with that in the initial functionalized LC polymer. Hydrogen bonding was detected for all the copolymers and blends investigated.

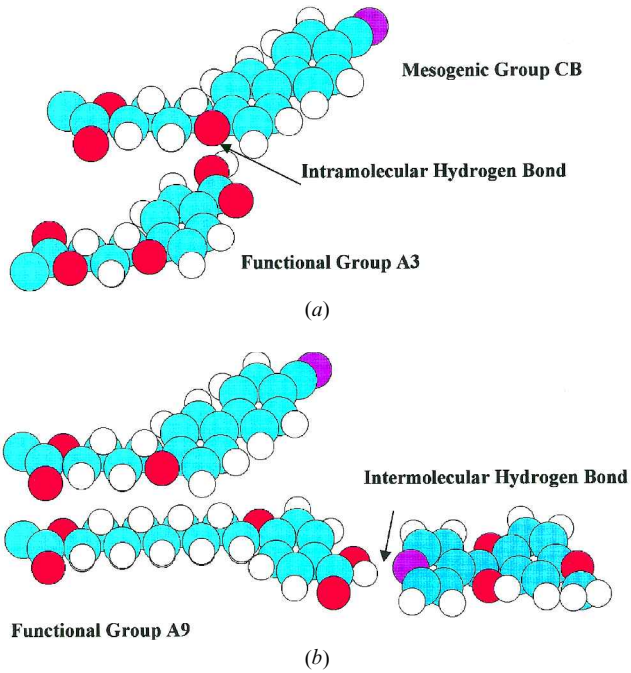

Figure 4. Sketch of the hydrogen bonding in the functionalized LC copolymer **P3** (*a*) and the blend **P3-PyOCH$_3$** (*b*). For simplicity the polymer main chain is not shown.

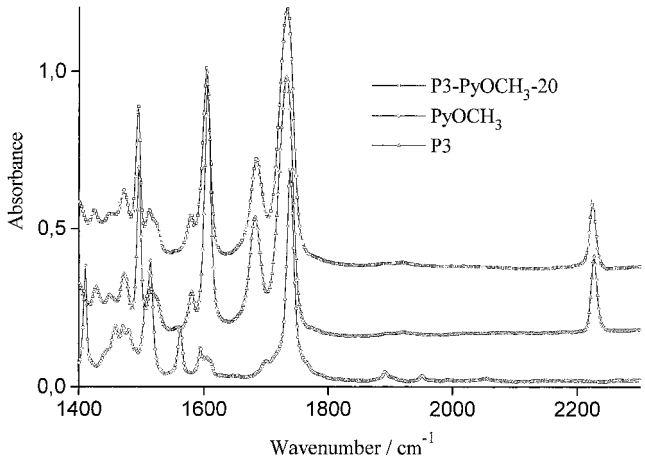

Figure 5. FTIR spectra of the functionalized LC copolymer **P3**, dopant **PyOCH$_3$** and blend **P3-PyOCH$_3$-20** at room temperature.

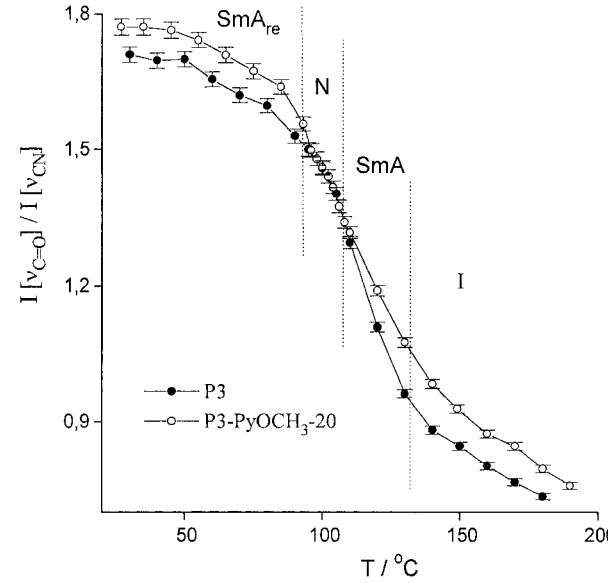

Figure 6. Temperature dependence of the intensity of the ratio $I[\nu_{C=O}]/I[\nu_{CN}]$ for the LC copolymer **P3** and the blend **P3-PyOCH$_3$-20**. The dashed lines correspond to the transition temperatures for blend **P3-PyOCH$_3$-20**.

3.2. *Birefringence and orientational elastic constants*

Figure 7 shows the temperature dependence of the birefringence Δn for the **P3-PyOCH$_3$** and **P3-PyCN** blends. The shape of these dependences is typical for LC polymers [14, 20–24] and low molar mass [25] nematics. As can be seen from figure 7, at the phase transition N↔SmA_{re} the value of Δn of the **P1-PyOCH$_3$** blend changes without any jump. Consequently, the order parameter S in the vicinity of this transition does not change in a jump-wise manner either. This behaviour of Δn at nematic–smectic transitions has been found by us previously for a number of side group polymers [22]. This may indicate that the transition under consideration has a second order character. However, it should be borne in mind that in the case of a weakly expressed first order transition (which can be the case for the transition from the nematic into the smectic A phase) the value of S and, hence, that of Δn do change very slightly. The possible jump in the order parameter can be within the experimental error in Δn which attains 4%.

The study of orientational elastic deformations in a magnetic field makes it possible to determine the phase behaviour of blends, in particular to establish precisely the formation of the nematic phase. We have shown that homeotropic and planar textures for the blends are retained throughout the range of the LC state, and it is known that bend deformations in the smectic A phase are forbidden [25]. This enables us to determine with great precision the temperatures of the phase transitions N↔SmA by studying the appearance (or disappearance) of the bend deformation at the interface of the nematic and smectic A phases. Observation of deformation patterns in a planar layer on passing from SmA into the N phase also makes it possible to determine the phase transition temperature. In fact, splay deformations in the SmA phase occur relatively readily, and the values of the constants K_1 are close to those in the N phase. However, the value itself for these deformations cannot be fixed by the optical method, because the reorientation angle of the director is very small in the case of magnetic field used. On passing from the SmA to the N phase, splay deformation increases sharply, enabling us to determine exactly the temperature of the corresponding phase transition. Good agreement was found between the temperatures of the N↔SmA phase transitions determined by POM and by observation of orientational elastic deformations in a magnetic field. It should be emphasized once more that the values of the elastic constants (and more precisely, the possibility that they can be measured) and the shape of their temperature dependence are the most important and irrefutable proof of nematic phase formation in the blends.

The temperature dependences of the splay elastic constant K_1 (figure 8) are typical for a nematic phase. For both blends shown, the $K_1/\Delta\chi$ ratio increases slowly

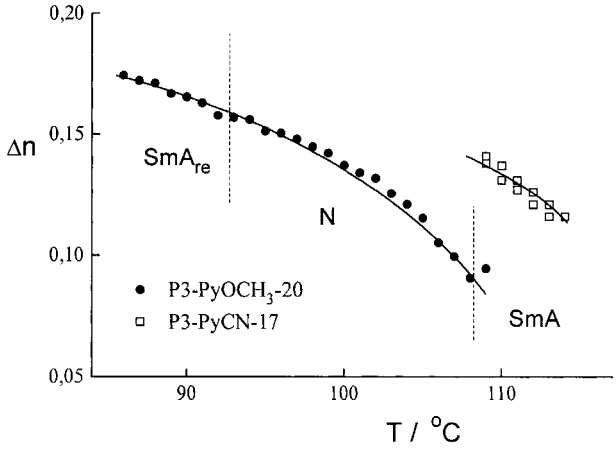

Figure 7. The birefringence Δn vs. temperature for the blends **P3-PyOCH$_3$-20** and **P3-PyCN-17**. The dashed lines correspond to the transition temperatures for blend **P3-PyOCH$_3$-20**.

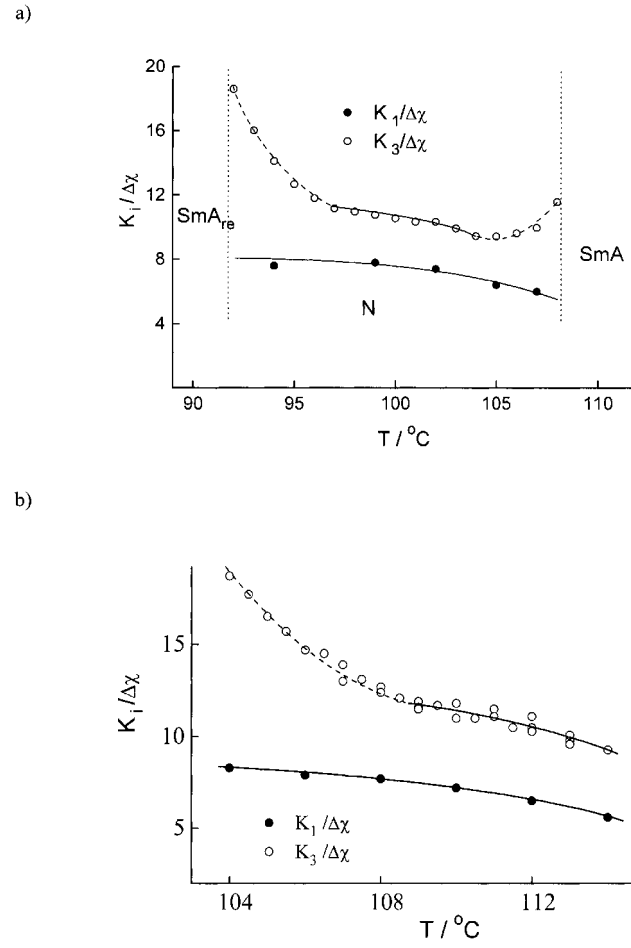

Figure 8. Dependences of the $K_3/\Delta\chi$ and $K_1/\Delta\chi$ ratios on temperature for the blends **P3-PyOCH$_3$-20** (*a*) and **P3-PyCN-17** (*b*).

with decreasing temperature. The temperature dependence of the bend elastic constant K_3 is quite different. At high temperatures the $K_3/\Delta\chi$ ratio for the **P3-PyOCH$_3$** blend slightly decreases with temperature. In the range from 105 to 96°C, the dependence has the usual 'nematic' shape. On further decrease of temperature, the $K_3/\Delta\chi$ ratio increases abruptly. Such a shape for the $K_3/\Delta\chi$ dependence on temperature may be explained by the appearance of smectic order fluctuations in the nematic phase near the transition into the SmA phase. Their appearance usually leads to a drastic increase in K_3 [25]. The increase in K_3 values near the transitions at the interface between the nematic and the SmA phases has previously been observed for common nematic [26] and re-entrant nematic [22] side group LC polymers.

For the **P3-PyCN** blend, the critical behaviour of the K_3 constant was observed only in the vicinity of the transition into the low temperature SmA phase. At higher temperatures near the N–SmA phase transition, no increase in $K_3/\Delta\chi$ was detected. This is probably due to the spontaneous transition‡ of the homeotropic orientation into a planar orientation at 114–115°C, which makes it impossible to carry out $K_i/\Delta\chi$ measurements in the nematic phase at these temperatures.

In the temperature range in which smectic order fluctuations are absent, experimental points corresponding to K_3 fall much higher than those for K_1, i.e. $K_3 > K_1$. Moreover, the K_3/K_1 ratio ranges from 1.3 to 1.5. This is much greater than the K_3/K_1 values (0.6–1.0) obtained for side group polymers with phenyl benzoate mesogenic groups [27].

This difference in the K_3/K_1 values may be associated with the distinction between the chemical structures of the mesogenic groups in the LC polymers and the blends. The K_3/K_1 value is known to depend strongly on the size and shape of the nematic molecules [25]. In the case of the LC polymers, the K_3/K_1 ratio is mainly determined by the size of mesogenic groups. This ratio grows with increasing ratio of the length to the thickness (breadth) of the mesogenic cores [14, 24]. Accordingly, the higher K_3/K_1 values obtained for the **P3-PyOCH$_3$** blend can be explained by the formation of new mesogenic groups due to hydrogen bonding between the dopant molecules and the functional groups of the **P3** copolymer. The length of the hydrogen-bonded group exceeds by almost one and a half times that of the mesogenic cores **CB** of the copolymer (figure 4). This leads to an increase in the mean 'effective' length of the mesogenic groups and to an increasing K_3/K_1 ratio. A similar effect of formation of hydrogen-bonded mesogenic groups on K_3/K_1 has been described in [10].

The $K_1/\Delta\chi$ and $K_3/\Delta\chi$ values for the blends are close in order of magnitude to those for ordinary and re-entrant phases of polymeric and low molar mass nematics. This indicates that for LC polymers with a covalent attachment of mesogenic groups and hydrogen-bonded molecules, the mesogenic group is the structural unit responsible for the equilibrium orientational elastic properties. Hence, with respect to orientational elastic deformations, the nematic phase in the hydrogen-bonded blends is comparable to that for copolymers in which the side groups are covalently bound to the polymer chain.

3.3. *Order parameter*

The Δn value for the LC blends characterizes only the average orientation of the optically anisotropic phenylene and pyridine rings located in the mesogenic and hydrogen-bonded fragments of the macromolecule. In other words, study of the birefringence does not provide complete information about the individual orientational behaviour of single fragments of the LC blends. Bearing in mind the complex blend structure, this information may however prove very useful for understanding physicochemical processes occurring in them. For example, the separate study of the orientational order of the dopant molecules **PyOCH$_3$** dissolved in the polymer matrix enables us to achieve two important things: (i) to obtain the value of the order parameter of the dopant S and the temperature dependence of S; (ii) to determine the temperature range of the dopant molecules in the liquid crystalline state. The new molecular fragment, figure 4 (*b*), is formed by hydrogen bonding; therefore it may be assumed that its thermostability should depend on temperature to a greater extent than does that of the cyanobiphenylyl mesogenic fragments. To elucidate these points, ^{2}H NMR spectroscopy was applied to the **PyOCH$_3$** dopant with a selectively deuteriated aromatic ring—4-methoxyphenyl-d$_4$ pyridine-4-carboxylate.

Figure 9 shows the temperature dependence of the ^{2}H NMR spectra for the **P3-PyOCH$_3$-20**. The transition from the isotropic melt into the nematic phase is realized through a biphasic region. This is supported by the intense central peak occurring in the 370–380 K temperature range, which corresponds to the isotropic phase of the **PyOCH$_3$** molecules. Two symmetric signals with a quadrupolar splitting parameter $\Delta\nu_q$ show that the dopant molecules are arranged in the ordered LC state.

‡ The spontaneous transition of one orientation into another (or the distortion of the homogeneous orientation in a sample) is usually considered to be related to a change in the balance of the forces of intermolecular interaction in a LC phase and the surface tension forces involving the solid support [25]. In this case, no independent information is available about the energy of the LC anchoring to the support. We can only assume that the anchoring changes at higher temperatures and leads to the observed spontaneous change in the director orientation.

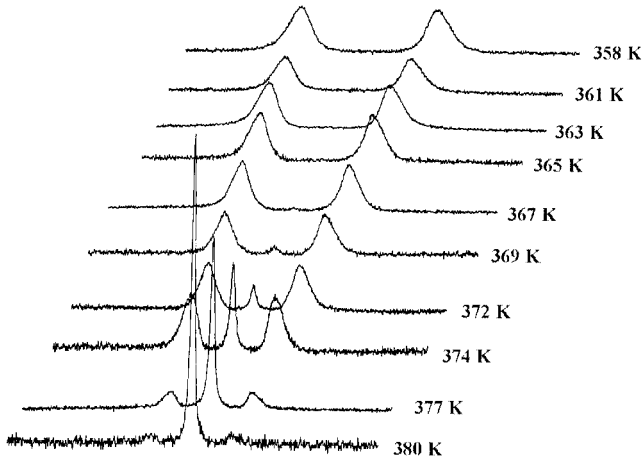

Figure 9. Temperature dependences of the ^{2}H NMR spectra for the blend **P3-PyOCH$_3$-20**.

The quadrupolar splitting ($\Delta\nu_q$) is determined by the geometry of the molecular unit ($\Delta\nu_{q0}$) and by the order parameter S: $\Delta\nu_q = \Delta\nu_{q0}S$. We calculated the local order parameter S with respect to the long axis of the dopant molecule that forms an angle of 14° with the *para*-axis ($\Delta\nu_{q0} = 22\,507$ Hz) and taking $D = 0$.

The temperature dependence of the order parameter S of the **PyOCH$_3$** molecules is shown in figure 10. The transition from the isotropic to the LC phase is accompanied by a jump in the order parameter to 0.25. Further temperature decrease leads to an increase in S. A similar temperature dependence of S is observed for the majority of low molar mass [25] and side group polymeric [28] liquid crystals.

It is seen that the transition from the nematic into the SmA and SmA_{re} phases is not accompanied by any marked change in the order parameter S. It should be recollected that the birefringence behaves in the same way, and literature data show that the order parameters of low molar mass liquid crystals change smoothly on passing from the SmA phase into the re-entrant nematic phase. This conclusion has been repeatedly confirmed by studies of the order parameter of LC blends by ESP [29], ^{2}H NMR [30], and optical birefringence [31]. Studies of re-entrant mesomorphism in side group LC polymers have also shown that with respect to physical properties, the re-entrant nematic phase is completely identical with the common nematic phase [22, 32].

^{2}H NMR spectroscopy also enables us to study the temperature range of the LC phase for the selectively deuteriated molecules **PyOCH$_3$**. The experimental procedure was very simple. The standard temperature dependence of the ^{2}H NMR spectra is recorded. The disappearance of the splitting $\Delta\nu$ and the appearance of a single narrow central peak in the ^{2}H NMR spectrum corresponds to the isotropic state. As can be seen from figure 9, the liquid crystalline to isotropic melt transition for the **P3-PyOCH$_3$** blend covers approximately 10°C. Figure 11 shows the temperature dependence of the content of nematic phase in the **P3-PyOCH$_3$** blend in

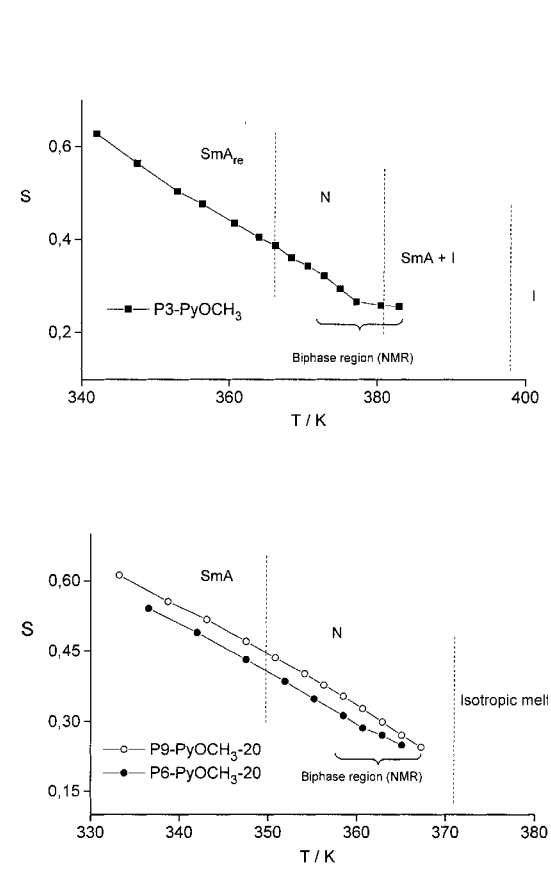

Figure 10. Temperature dependences of the order parameter S for the blends **P3-PyOCH$_3$-20** (*a*) and **P6-PyOCH$_3$-20** and **P9-PyOCH$_3$-20** (*b*). The dashed lines correspond to the transition temperatures measured by polarizing optical microscopy.

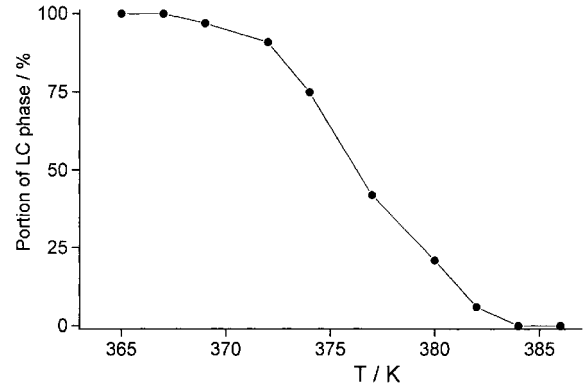

Figure 11. The proportion of the dopant **PyOCH$_3$** in liquid crystalline phase formed in the blends **P3-RyOCH$_3$-20** in the biphasic region (nematic and isotropic melt).

the biphasic region. This dependence was obtained by integrating the signals for the isotropic and LC parts of the ^{2}H NMR spectra.

Attention is mainly drawn to the discrepancy between the clearing temperatures obtained by NMR spectroscopy (points in figure 10) and by POM (broken line in figure 10). The difference is about 10°C, which is much greater than the experimental errors of these methods. This discrepancy arises because ^{2}H NMR spectroscopy gives the distortion temperature for the long range orientational order of the molecules of **PyOCH$_3$** dopant. This process may be called the orientational melting of the dopant by analogy with the distortion of orientational order according to the Pople–Karasz model [33]. On the other hand, POM does not fix the melting of the mesophase. For example, at 106°C a typical nematic marble texture is recorded, figure 3 (*e*). However, according to ^{2}H NMR spectroscopy, at this temperature $\sim$70% of the dopant molecules are in the molten state, figure 11.

Consequently, we have detected an interesting phenomenon. At a certain temperature in the hydrogen-bonded LC blends the molecules of the **PyOCH$_3$** dopant undergo melting. At the same time, over a relatively wide temperature range, the blend remains liquid crystalline as a whole, as evidenced by all data obtained by POM, figure 3, and by studies of the orientational elastic deformations in a magnetic field, figure 8 (*a*).

The orientational behaviour of the dopant discussed above is possible only in the case where the **Py*R*** molecules are segregated into an individual microphase which has all the complex range of properties of the mesophase. The evidence for this is the jump-like change in the order parameter S. Thus the liquid crystal–isotropic phase transition is a first order phase transition. At the same time, for a continuous phase, the non-zero order parameter of the dopant molecules must be retained over all the LC phase range (for example, by a 'guest–host' mechanism). The absence of macroscopic phase separation as discussed above shows that the regions of agregated dopant molecules are not large. It seems that regions with a local high dopant molecular concentration are augmented during the process of blend preparation and rather quickly reach equilibrium values during the subsequent temperature treatment. It must be said that the tendency to microsegregation of macromolecular fragments of different chemical nature and polarity often predetermines the properties and structure of side group LC polymers. For functionalized LC copolymers this tendency must be expressed even more strongly.

Let us consider the effect of the chemical structure of the functionalized LC copolymers on the order parameter of the **PyOCH$_3$** dopant. It was established that S(**P3-PyOCH$_3$**) $\approx S$(**P6-PyOCH$_3$**) $< S$(**P9-PyOCH$_3$**). In other words, the order parameter S depends on the length of the aliphatic spacer in the functionalized LC polymer. Increase in the spacer length n leads to a marked increase in S due to the different steric environments of the hydrogen-bonded complex. When the spacer lengths are $n = 3$ and 6, the length of a functional monomer containing a free carboxyl group is smaller than that of the cyanobiphenylyl mesogenic fragment **CB**. Hence, the mesogenic groups **CB** of the copolymer matrix of **P3** and **P6** prevent the optimal orientation of **PyOCH$_3$**. For copolymer **P9** ($n = 9$), the length L of the functional monomer ($L = 21$ Å) is only slightly greater than that of the **CB** fragment ($L = 18$ Å). Therefore, steric conditions for the formation of a hydrogen-bonded complex are improved and lead to still higher values of the order parameter S of the dopant molecules **PyOCH$_3$**.

3.4. *Mechanism of the nematic phase formation in the hydrogen-bonded blends*

It should be noted that the observed phase behaviour of the blends is difficult to predict and is a rather unusual phenomenon. In fact, according to figure 4 (*b*), a new hydrogen-bonded molecule with a high degree of anisodiametry had to be formed in the blends of the *n*-alkyloxybenzoic acids with the pyridine-containing groups. The formation of a new extended molecule according to Kato and Frechet [1] is accompanied by an increasing clearing temperature T_C of the blend with a characteristic maximum in T_C at the equimolar composition of the complex. Moreover, induction of smectic phases was observed in the blends, although the initial components were nematics or even did not exhibit any mesomorphic properties.

The blends of the functionalized LC polymers **P3**, **P6** and **P9** with the **Py*R*** dopant exhibit the opposite tendency. The addition of a non-mesogenic dopant **Py*R*** to the smectic polymer induces the appearance of the nematic phase and gives an essential decrease in thermal stability.

In a preliminary study of re-entrant mesomorphism in the polymer blends **P3-PyCN** [11], it has already been suggested that hydrogen bonds play an important role in the appearance of the N and SmA_{re} phases. The present study has shown that in addition to hydrogen bonds, the chemical structure of the polymer matrix also influences the situation. In fact, the phase sequence I–SmA–N–SmA_{re} is given only in the blends with the polymer **P3** in which the spacer length $n = 3$. Longer spacers ($n = 6$ and 9) cause the formation of common nematic and smectic phases (I–N–SmA). Furthermore, it was found that the polarity of the **Py*R*** dopant molecule has virtually no effect on the formation of nematic properties and re-entrant mesomorphism.

For the first time the N and SmA_{re} phases were observed in the blends of polymer **P3** with the molecules of the **PyCN** dopant containing the strongly polar cyano group ($\mu \sim 4$ D). It is shown in this work however that the same effect is observed when the CN groups are replaced by weakly polar methoxy OCH_3 groups ($\mu \sim 1$ D). Hence, it may be concluded that the formation of the nematic phase in the blends depends on the type of the functionalized LC polymer and does not depend on the polarity of the terminal group of the **Py*R*** dopant molecule.

Before passing to an explanation of the reason for the I–SmA–N–SmA_{re} phase sequence, we should consider the conditions favouring the distortion of the SmA phase of the copolymer and the induction of the nematic phase that is present in all blends. The distortion of the smectic phase is due to the formation of a new hydrogen-bonded molecule, figure 4(*b*); this results from the fact that the formation of the hydrogen-bonded mesogenic group changes the system of intra- and inter-molecular hydrogen bonds established in the LC copolymers **P3–P9** and necessary for SmA phase formation.

As shown in [10], the main difference between the copolymers **P3–P9** is the different character of their hydrogen bonds. Copolymers **P6** and **P9** form intermolecular hydrogen bonds, whereas **P3** forms intramolecular bonds; see figure 4(*a*). Smectic phase formation in the copolymers **P6** and **P9** is possible only in the case where the functional carboxyl groups **A6** and **A9** of the copolymers form intermolecular hydrogen bonds. This phenomenon is accounted for by the fact that only in the dimer form do the **A6** and **A9** molecules exhibit mesomorphic properties. Since the initial homopolymer **CB** is nematic, the smectic phase in the copolymers **P6** and **P9** is caused by the units of the functional monomer and the homopolymer which together form the SmA phase. An opposite situation is observed for the polymer **P3** in which the SmA phase is formed due to the intramolecular hydrogen bonds between the monomer unit **A3** and the oxygen of the ether bond of the mesogenic fragment **CB**; see figure 4(*a*). Intramolecular hydrogen bonds lead to the formation of a fragmentary ladder-like structure giving increasing polymer rigidity. The intramolecular character of hydrogen bonds is reflected in the transition temperatures of the LC copolymers. The table shows that for similar degrees of polymerization, the copolymer **P3** has a relatively high glass transition (49°C) and clearing temperature (~140°C), whereas the polymers **P6** and **P9** have much lower transition temperatures.

It is evident that the incorporation of dopant molecules **Py*R*** into the LC copolymers **P6** and **P9** prevents the formation of intermolecular hydrogen bonds between the carboxylic groups of the functional monomer. At the same time the copolymer **P3** in the blend **P3-Py*R*** retains the possibility of forming intramolecular hydrogen bonds. Their formation is mainly determined by the configurational chain structure (the distribution of the mesogenic **CB** and functional **A3** monomers in the molecule of the copolymer **P3**)§.

Moreover, nematic phase induction also occurs because of the overall decrease in the order of the blend resulting from the lower values of the order parameter of the **Py*R*** dopant molecules as compared with the mesogenic side groups. This conclusion does not follow directly from the results of the present investigation, but from [34], which considered the order parameter of **$PyOCH_3$** dopant dissolved in a functionalized polymer matrix with selectively deuteriated phenyl benzoate mesogenic fragments. Hence, this work reports two reasons for the perturbation of the smectic packing of the mesogenic side groups and of the induction of the nematic phase. The next step will be the explanation of the conditions causing the formation of the high temperature smectic phase in the **P3-$PyOCH_3$** and **P3-PyCN** blends and its absence in the **P6-$PyOCH_3$** and **P9-$PyOCH_3$** blends.

The following explanation of the nematic phase distortion and the appearance of the high temperature SmA phase in the **P3-Py*R*** polymer blends may be suggested. Temperature increase leads to melting of the **Py*R*** dopant molecules. Hence, conditions favouring nematic phase formation in the **P3-Py*R*** blends disappear. Under these conditions the molecules of the **Py*R*** dopant play only the role of a plasticizer. At the same time owing to intramolecular hydrogen bonds, the copolymer **P3** retains a sufficient thermal stability. In the pure state (without dopant), **P3** forms the SmA phase with $T_C = 140$°C. Hence, the blends also forms the high temperature SmA phase. In other words, common plasticization of a smectic polymer by a low molecular mass dopant **Py*R*** takes place, and it is known that plasticizers lead to decrease in transition temperatures, but the phase state usually does not change.

Consequently, two main contributions leading to the formation of the high temperature SmA phase can be singled out: (i) internal (natural) rigidity of the polymer matrix **P3**; (ii) destruction of the new hydrogen-bonded mesogenic group, figure 4(*b*), with increasing temperature (orientational melting).

§It is well known [19] that the essential difference between intra- and inter-molecular hydrogen bonds is the fact that the latter break when solutions are diluted with a nonapolar solvent, whereas intramolecular hydrogen bonds do not depend on solution concentration. An appropriate analogy can be drawn between the behaviour of hydrogen bonds upon dilution and that of the blends studied in our work and obtained by 'dilution' of functionalized LC polymers with a 'solvent', a low-molar-mass dopant **Py*R***.

For **P6-PyOCH$_3$-20** and **P9-PyOCH$_3$-20** blends, the dopant molecules **PyOCH$_3$** melt at 76–94°C. At the same time, the formation of intermolecular hydrogen bonds is hindered between the carboxyl groups accountable for the smectic phase formation. Hence, the distortion of the hydrogen-bonded mesogenic group and the plasticization of the blend is completed by total melting of the nematic phase ($T_C = 100$°C for **P6-PyOCH$_3$-20** and 97°C for **P9-PyOCH$_3$-20**).

The main reason leading to the appearance of the nematic and re-entrant smectic phases is a complex of steric factors. They appear because of the complicated structure of a side group LC copolymer and the different types of hydrogen bonds in the blends. Therefore, according to the nomenclature for re-entrant phases [35], the observed phase may be placed in class R2—'re-entrance from geometric complexity'.

4. Conclusion

New hydrogen-bonded blends of functionalized LC polymers containing acid groups (proton donors) with proton acceptor dopants have been obtained. It was shown that new mesogenic groups are formed by intermolecular hydrogen bonding between the dopant molecules **Py*R*** and the carboxyl groups of the functionalized LC copolymer.

An unusual phenomenon was found: the formation of hydrogen-bonded blends leads to the destruction of the smectic phase of the functionalized LC copolymers and the formation of nematic and re-entrant smectic phases. The effect of the dopant concentration and polarity, as well as of the chemical structure of the polymer matrix on the formation of the N and SmA_{re} phases in the blends was studied.

Orientational elastic properties of the nematic phase were studied, and the temperature dependences of the elastic constants K_1 and K_3 and the birefringence Δn were obtained. The orientation of the dopant molecules was studied by ^{2}H NMR spectroscopy. Selective melting of the dopant molecules **PyOCH$_3$** in the blends (orientational melting) was detected. This involves the dopant order parameter dropping to zero, whereas the copolymer matrix is in the liquid crystalline state and macroscopic phase separation is not observed.

A mechanism for the formation of the N and SmA_{re} phases in the LC polymer blends is proposed. It takes into account the chain rigidity of the functionalized LC copolymers and the orientational melting of the dopant molecules.

This research has been supported personally (to E. B. Barmatov) by the Alexander von Humboldt Foundation (Germany) and the RFBR (Grant nn. 98-03-33390).

References

[1] Kato, T., and Frechet, M. J., 1989, *J. Am. Chem. Soc.*, **111,** 8533.

[2] Kresse, H., Szulzewsky, I., Diele, S., and Paschke, R., 1994, *Mol. Cryst. Liq. Cryst.*, **238,** 19; Bernhardt, H., Weissflog, W., and Kresse, H., 1998, *Liq. Cryst.*, **24,** 895.

[3] He, C., Donald, A. M., Griffin, A. C., Waigh, T., and Windle, A. H., 1998, *J. Polym. Sci., B*, **36,** 1617.

[4] Kihara, H., Kato, T., Uryu, T., Ujiie, S., Kumar, U., Frechet, J. M. J., Bruce, D. W., and Price, D. J., 1996, *Liq. Cryst.*, **21,** 25.

[5] Kato, T., and Frechet, M. J., 1995, *Macromol. Symp.*, **98,** 311; Kato, T., 1997, in *Handbook of Liquid Crystals*, Vol. 2B, edited by D. Demus, J. Goodby, G. W. Gray, H.-W. Spiess, and V. Vill (Weinheim: Wiley-VCH), p. 969.

[6] Paleos, C. M., and Tsiourvas, D., 1995, *Angew. Chem. Int. Ed. Engl.*, **34,** 1696; Ujiie, S., and Iimura, K., 1992, *Macromolecules*, **25,** 3174; Wiesemann, A., Zentel, R., and Pakula, T., 1992, *Polymer*, **33,** 5315; Zhao, Y., and Lei, H., 1994, *Macromolecules*, **27,** 4225; Kosaka, Y., and Uryu, T., 1994, *Macromolecules*, **27,** 6286.

[7] Barmatov, E. B., Barmatova, M. V., Chenskay, T. B., and Shibaev, V. P., 1999, *Polym. Sci.*, **41,** 337; Barmatov, E. B., Pebalk, D. A., Barmatova, M. V., and Shibaev, V. P., 1999, *Polym. Sci.*, **41,** 824; Barmatov, E. B., Barmatova, M. V., Chenskay, T. B., and Shibaev, V. P., 1999, *Mol. Cryst. Liq. Cryst.*, **332,** 2941; Barmatov, E., Pebalk, D., Barmatova, M., and Shibaev, V., 2000, *Macromol. Rapid Commun.*, **21,** 369; Barmatov, E., Prosvirin, A., Barmatova, M., Galyametdinov, Yu., Haase, W., and Shibaev, V., 2000, *Macromol. Rapid Commun.*, **21,** 281.

[8] Barmatov, E. B., Pebalk, D. A., Barmatova, M. V., and Shibaev, V. P., 1997, *Liq. Cryst.*, **23,** 447; Barmatov, E. B., Barmatova, M. V., Grokhovskaya, T. E., and Shibaev, V. P., 1998, *Polym. Sci.*, **40,** 295; Shibaev, V. P., Barmatov, E. B., and Barmatova, M. V., 1998, *Col. Polym. Sci.*, 276, 662; Barmatov, E., Barmatova, M., Kremer, F., and Shibaev, V., 2000, *Macromol. Chem. Phys.*, **201,** 13.

[9] Barmatov, E. B., Bobrovsky, A. Yu., Barmatova, M. V., and Shibaev, V. P., 1998, *Polym. Sci.*, **40,** 1769; Barmatov, E. B., Bobrovsky, A. Yu., Barmatova, M. V., and Shibaev, V. P., 1999, *Liq. Cryst.*, **26,** 581; Barmatov, E. B., Bobrovsky, A. Yu., Pebalk, D. A., Barmatova, M. V., and Shibaev, V. P., 1999, *J. Polym. Sci. A: Polym. Chem.*, **37,** 3215.

[10] Filippov, A. P., Andreeva, L. N., Barmatov, E. B., Barmatova, M. V., Grande, S., Kremer, F., and Shibaev, V. P., 2000, *Polym. Sci.*, **42,** 329; Filippov, A., Andreeva, L., Barmatov, E., Barmatova, M., Kremer, F., and Shibaev, V., 2000, *Macromol. Chem. Phys.*, **201,** 2591.

[11] Barmatov, E., Filippov, A., Andreeva, L., Barmatova, M., Kremer, F., and Shibaev, V., 1999, *Macromol. Rapid Commun.*, **20,** 521.

[12] Freedericksz, V. K., and Zolina, V. V., 1931, *Z. Kristallogr.*, **79,** 255.

[13] Tsvetkov, V. N., and Kolomiets, I. P., 1988, *Mol. Cryst. Liq. Cryst.*, **157,** 467.

[14] Andreeva, L. N., Filippov, A. P., Tsvetkov, V. N., and Bilibin, A. Yu., 1998, *Polym. Sci.*, **40,** 124.
[15] Ruhmann, R., Thiele, T., Prescher, D., and Wolff, D., 1995, *Macromol. Rapid Commun.*, **16,** 161; Kostromin, S. G., and Shibaev, V. P., 1999, *Polym. Sci.*, **41,** 346.
[16] Gubina, T. I., Kostromin, S. G., Tal'roze, R. V., Shibaev, V. P., and Plate, N. A., 1986, *Vysokomol. Soedin. B.*, **28,** 394.
[17] Emmerling, U., Diele, S., Schmalfuss, H., Werner, J., Kresse, H., and Lindau, J., 1998, *Macromol. Chem. Phys.*, **199,** 1529.
[18] Freidzon, Ya. S., Boiko, N. I., Shibaev, V. P., and Plate, N. A., 1987, *Vysokomol. Soedin. A.*, **29,** 934.
[19] Smith, A., and Lee, 1979, *Applied Infrared Spectroscopy* (New York: John Wiley).
[20] Tsvetkov, V. N., Andreeva, L. N., Filippov, A. P., Smirnova, G. S., Skorokhodov, S. S., and Bilibin, A. Yu., 1992, *Poly. Sci.*, **34,** 615.
[21] Andreeva, L. N., Filippov, A. P., Tsvetkov, V. N., Zuev, V. V., Skorokhodov, S. S., Zentel, R., and Poths, H., 1994, *Eur. Polym. J.*, **30,** 1461.
[22] Filippov, A. P., Andreeva, L. N., Barmatov, E. B., and Shibaev, V. P., 1997, *Proc. SPIE*, **3218,** 371.
[23] Filippov, A. P., Andreeva, L. N., Beljaeva, E. V., Barmatov, E. B., and Shibaev, V. P., 1999, *Mol. Cryst. Liq. Cryst.*, **330,** 183.
[24] Andreeva, L. N., Filippov, A. P., Tsvetkov, V. N., and Bilibin, A. Yu., 1999, *Mol. Cryst. liq. Cryst.*, **330,** 191.
[25] De Jeu, W. H., 1980, *Physical Properties of Liquid Crystalline Materials* (New York: Gordon & Breach).
[26] Filippov, A. P., and Zuev, V. V., 1999, *Macromol. Rapid Commun.*, **20,** 552.
[27] Andreeva, L. N., Filippov, A. P., Tsvetkov, V. N., Barmatov, E. B., and Shibaev, V. P., 1997, *Polym. Sci.*, **39,** 714.
[28] Shibaev, V. P., Barmatov, E. B., and Stroganov, L. B., 1993, in *Modern Topics in Liquid Crystals* edited by A. Buka (Singapore: World Scientific), p. 73; Barmatov, E. B., Stroganov, L. B., Talroze, R. V., Shibaev, V. P., and Plate, N. A., 1993, *Polym. Sci.*, **35,** 183; Barmatov, E. B., Boiko, N. I., and Shibaev, V. P., 1997, *Polym. Sci.*, **39,** 582; Holstein, P., Barmatov, E. B., Geschke, D., Bender, M., and Shibaev, V. P., 2000, *Col. Polym. Sci.*, **278,** 711.
[29] Luckhurst, G. R., Smith, K. J., and Timimi, B. A., 1980, *Mol. Cryst. Liq. Cryst. Lett.*, **56,** 315.
[30] Hafiz, N., Vaz, N. A. P., Yaniv, Z., Allender, D., and Doane, J. W., 1982, *Phys. Lett. A*, **91,** 411; Emsley, J. W., Luckhurst, G. R., Parsons, P. J., and Timimi, B. A., 1985, *Mol. Phys.*, **56,** 767.
[31] Chen, N. S., Hark, S. K., and Ho, J. T., 1981, *Phys. Rev. A*, **24,** 2843.
[32] Kireev, E. V., Stroganov, L. B., Gubina, T. I., Kostromin, S. G., Talroze, R. V., Shibaev, V. P., and Plate, N. A., 1989, *Vysokomol. Soedin. B*, **31,** 216.
[33] Pople, A., and Karasz, F. E., 1961, *J. Phys. Chem. Solids*, **18,** 28; Pople, J. A., and Karasz, F. E., 1961, *J. Phys. Chem. Solids*, **20,** 294.
[34] Barmatov, E., Grande, S., Filippov, A., Barmatova, M., Kremer, F., and Shibaev, V., 2000, *Macromol. Chem. Phys.*, **201,** 2603; Filippov, A. P., Andropov, V. V., Barmatov, E. B., Kremer, F., Barmatova, M. V., and Shibaev, V. P., 2000, *Liq. Cryst.*, **27,** 1585.
[35] Cladis, P. E., in *Handbook of Liquid Crystals*, edited by D. Demus, J. Goodby, G. W. Gray, H.-W. Spiess, and V. Vill (Weinheim: Wiley-VCH), p. 391.